Chapter 2

An efficient fitted mesh method for coupled systems of singularly perturbed delay problems

In this chapter, we consider the following parabolic delay system having different perturbation parameters

$$\mathcal{L}\boldsymbol{u}(x,t) := \boldsymbol{L}\boldsymbol{u}(x,t) + \boldsymbol{B}\boldsymbol{u}(x,t-\tau) = \boldsymbol{f}(x,t), \quad (x,t) \in \Omega = D \times (0,T], \tag{2.1}$$

subject to initial and boundary conditions

$$\begin{cases} \boldsymbol{u}(0,t) = \mathbf{g}_\ell(t), \quad \boldsymbol{u}(1,t) = \mathbf{g}_r(t), \quad 0 < t \leq T, \\ \boldsymbol{u}(x,t) = \mathbf{g}_b(x,t), \quad 0 \leq x \leq 1, \quad -\tau \leq t \leq 0, \end{cases}$$

with

$$\boldsymbol{L}\boldsymbol{u}(x,t) = \partial_t \boldsymbol{u}(x,t) - \boldsymbol{\mathcal{E}}\partial_x^2 \boldsymbol{u}(x,t) + \boldsymbol{A}\boldsymbol{u}(x,t),$$

where

$$\boldsymbol{\mathcal{E}} = \begin{pmatrix} \varepsilon_1 & 0 \\ 0 & \varepsilon_2 \end{pmatrix}, \ \boldsymbol{A} = \begin{pmatrix} a_{11}(x,t) & a_{12}(x,t) \\ a_{21}(x,t) & a_{22}(x,t) \end{pmatrix}, \ \boldsymbol{B} = \begin{pmatrix} b_{11}(x,t) & b_{12}(x,t) \\ b_{21}(x,t) & b_{22}(x,t) \end{pmatrix}, \ \boldsymbol{f} = \begin{pmatrix} f_1 \\ f_2 \end{pmatrix}.$$

The entries of matrices $\boldsymbol{A}$ and $\boldsymbol{B}$ satisfy

$$\begin{cases} a_{ij} \leq 0, \quad i \neq j; \ |b_{ij}| \leq \beta, \ i,j = 1,2, \\ a_{ii} > 0, \quad \sum_{j=1}^{2} a_{ij} \geq \alpha > 0, \ i = 1,2. \end{cases}$$

We define $\boldsymbol{\Gamma} = \boldsymbol{\Gamma}_b \cup \boldsymbol{\Gamma}_\ell \cup \boldsymbol{\Gamma}_r$, where $\boldsymbol{\Gamma}_\ell$ and $\boldsymbol{\Gamma}_r$ represent the left and the right boundaries of the domain Ω and $\boldsymbol{\Gamma}_b = \overline{D} \times [-\tau, 0]$, $D = (0,1)$. Further, we define $T = n\tau$ for some positive integer n. The data of problem (2.1) is supposed to be enough smooth and satisfies compatibility conditions in order that $\boldsymbol{u} \in C^{4,2}(\overline{\Omega})^2$ [94, 95]. The parameters $\varepsilon_i, i = 1,2$, are such that $0 < \varepsilon_1 \leq \varepsilon_2 \leq 1$.

Robust numerical methods for scalar singularly perturbed delay ordinary differential equations (ODEs) and partial differential equations (PDEs) have also been developed extensively in the literature, see e.g. [96–100] for ODEs and [91, 101–106] for PDEs. In particular, for a scalar singularly perturbed parabolic partial differential equation with time delay, the authors in [101] provided a robust numerical method by discretizing the problem using a finite difference scheme on a Shishkin mesh. The authors in [103] developed a robust domain decomposition method of Schwarz waveform relaxation type. The authors in [102] developed a fitted operator method. In spite of these interesting research available in literature on singularly perturbed delay differential equations, the work related to the numerical solution of systems of singularly perturbed delay differential equations is still at infant stage.

The main purpose of this chapter is to develop an adaptive numerical method for problem (2.1). The current work utilizes two splitting schemes [107] that decouple the components of the approximate solution at each time level and hence resulted in a reduced computational time. To approximate the solution of the problem, we consider two splitting schemes on uniform meshes for time discretization and the

central difference scheme on Shishkin and generalised Shishkin meshes for space discretization. It is shown that the proposed numerical method is robust convergent of order one in time and almost two in space. Further, the CPU time comparison shows that the splitting schemes are computationally more efficient than the classical backward Euler scheme [52].

This work is arranged as follows. We describe the splitting schemes based numerical method for problem (2.1) in Section 2.2. Convergence analysis of the numerical method is discussed in Section 2.3. In Section 2.4, numerical results are reported which confirm the theory and efficiency of the proposed numerical method. Finally, conclusions are given in Section 2.5.

2.1 A priori bounds on the solution derivatives

In this section, we derive a priori bound for the exact solution of problem (2.1) and its derivatives. These bounds will be used later in defining layer adapted meshes and to derive error estimates for the proposed numerical method. To deduce the appropriate a priori bound we frequently use the following maximum principle result, which can be proved using the standard arguments [54, 108].

Lemma 2.1. *If* $\boldsymbol{z}(x,t) \geq \mathbf{0}$, *for* $(x,t) \in \boldsymbol{\Gamma}$ *and* $\boldsymbol{L}\boldsymbol{z}(x,t) \geq \mathbf{0}$, *for* $(x,t) \in \Omega$, *then* $\boldsymbol{z}(x,t) \geq \mathbf{0}$, *for* $(x,t) \in \overline{\Omega}$.

The following comparison principle result is an immediate consequence of the above maximum principle.

Corollary 2.2. *If* $|\boldsymbol{\psi}(x,t)| \leq \boldsymbol{\varphi}(x,t)$, *for* $(x,t) \in \boldsymbol{\Gamma}$ *and* $|\boldsymbol{L}\boldsymbol{\psi}(x,t)| \leq \boldsymbol{L}\boldsymbol{\varphi}(x,t)$, *for* $(x,t) \in \Omega$, *then* $|\boldsymbol{\psi}(x,t)| \leq \boldsymbol{\varphi}(x,t)$ *for* $(x,t) \in \overline{\Omega}$.

Lemma 2.3. *The solution of problem (2.1) satisfies*

$$\|\partial_t^s u_\ell\|_{\overline{\Omega}} \leq C, \quad \textit{for} \;\; s = 0, 1, 2, \quad \ell = 1, 2.$$

Proof. We first prove the result for $t \in (0, \tau]$ using mathematical induction on s. Set $\boldsymbol{\varphi} = \boldsymbol{C}(1 + t)$, then result for $s = 0$ follows using the barrier function $\boldsymbol{\varphi}$ with the comparison principle result for $\boldsymbol{L}$. In the hypothesis step, we assume that the result holds for $s = 0, \ldots, \kappa - 1$, $1 \leq \kappa \leq 2$. Next, we need to prove the result for $s = \kappa$. Defining $\boldsymbol{\Psi} = \partial_t^\kappa \boldsymbol{u}$, it holds

$$\begin{cases} \boldsymbol{L}\boldsymbol{\Psi}(x,t) := \partial_t \boldsymbol{\Psi}(x,t) - \boldsymbol{\mathcal{E}}\partial_x^2 \boldsymbol{\Psi}(x,t) + \boldsymbol{A}\boldsymbol{\Psi}(x,t) \\ \qquad\qquad = \partial_t^\kappa \boldsymbol{f}(x,t) - \sum_{l=0}^{\kappa-1} \binom{\kappa}{l} \boldsymbol{A}_t^{\kappa-l} \partial_t^l \boldsymbol{u}(x,t) - \sum_{l=0}^{\kappa} \binom{\kappa}{l} \boldsymbol{B}_t^{\kappa-l} \partial_t^l \boldsymbol{u}(x, t-\tau) \\ \qquad\qquad := \boldsymbol{\Psi}_\kappa \;\; \text{in } \Omega_1 = (0,1) \times (0, \tau], \end{cases}$$

and

$$\begin{cases} |\boldsymbol{\Psi}(x,0)| \leq \boldsymbol{C} \;\; \text{in } \overline{D}, \\ |\boldsymbol{\Psi}(x,t)| \leq \max\{|\mathbf{g}_\ell^{(\kappa)}(t)|, |\mathbf{g}_r^{(\kappa)}(t)|\} \leq \boldsymbol{C} \;\; \text{for } (x,t) \in \{0,1\} \times (0, \tau], \end{cases}$$

where the above boundary estimates follows from the assumption on data of problem (2.1). Now using inductive hypothesis we get $|\boldsymbol{\Psi}_\kappa(x,t)| \leq \boldsymbol{L}\boldsymbol{\varphi}(x,t)$. Thus, we get the required result using the comparison principle together with the barrier function $\boldsymbol{\varphi}$. So, we have the result on the domain $[0,1] \times [0, \tau]$. For $t \in (\tau, 2\tau]$, $\boldsymbol{u}$ is a solution of $\boldsymbol{L}\boldsymbol{u}(x,t) = \boldsymbol{F}(x,t)$, $(x,t) \in \Omega_2 = D \times (\tau, 2\tau]$, where $\boldsymbol{F}(x,t) = \boldsymbol{f}(x,t) - \boldsymbol{B}\boldsymbol{u}(x, t-\tau)$. So, we use the barrier function $\boldsymbol{\varphi} = \boldsymbol{C}(1 + t)$ with $\boldsymbol{C}$ a sufficiently large positive constant together with the comparison principle and the previous arguments to obtain $\|\partial_t^s u_\ell\|_{\overline{\Omega}_2} \leq C$, for $s = 0, 1, 2$, $\ell = 1, 2$, where $\Omega_2 = D \times (\tau, 2\tau]$. Finally, the result is proved using mathematical induction. □

Now we decompose the solution of problem (2.1) as $\boldsymbol{u} = \boldsymbol{v} + \boldsymbol{w}$, where $\boldsymbol{v}$ is the regular part and $\boldsymbol{w}$ is the singular part of the solution. The regular part is the solution of the problem

$$\begin{cases} \boldsymbol{L}\boldsymbol{v}(x,t) + \boldsymbol{B}\boldsymbol{v}(x,t-\tau) = \boldsymbol{f}(x,t) & \text{for } (x,t) \in \Omega, \\ \boldsymbol{v}(x,t) = \mathbf{g}_b(x,t) & \text{for } (x,t) \in \boldsymbol{\Gamma}_b, \\ \boldsymbol{v}(x,t) = \boldsymbol{\chi}(x,t) & \text{for } (x,t) \in \boldsymbol{\Gamma}_\ell \cup \boldsymbol{\Gamma}_r, \end{cases} \tag{2.2}$$

and the singular part is the solution of the problem

$$\begin{cases} \boldsymbol{L}\boldsymbol{w}(x,t) + \boldsymbol{B}\boldsymbol{w}(x,t-\tau) = \mathbf{0} & \text{for } (x,t) \in \Omega, \\ \boldsymbol{w}(x,t) = (\boldsymbol{u}-\boldsymbol{v})(x,t) & \text{for } (x,t) \in \boldsymbol{\Gamma}, \end{cases} \tag{2.3}$$

where $\boldsymbol{\chi}$ is the solution of the problem

$$\begin{cases} \partial_t \boldsymbol{\chi}(x,t) + \boldsymbol{A}\boldsymbol{\chi}(x,t) + \boldsymbol{B}\boldsymbol{\chi}(x,t-\tau) = \boldsymbol{f}(x,t), & (x,t) \in \boldsymbol{\Gamma}_\ell \cup \boldsymbol{\Gamma}_r, \\ \boldsymbol{\chi}(x,t) = \mathbf{g}_b(x,t), & (x,t) \in \boldsymbol{\Gamma}_b. \end{cases} \tag{2.4}$$

Lemma 2.4. *The solution $\boldsymbol{v}$ of problem (2.2) satisfies*

$$\|\partial_t^s v_\ell\|_{\overline{\Omega}} \leq C \quad \textit{for} \quad s = 0,1,2, \ \ell = 1,2. \tag{2.5}$$

$$\|\partial_x^s v_\ell\|_{\overline{\Omega}} \leq C(1+\varepsilon_\ell^{1-s/2}) \quad \textit{for} \quad s = 1,2,3,4, \ \ell = 1,2. \tag{2.6}$$

Proof. The proof of (2.5) follows using similar arguments as in the proof of Lemma 2.3. We next establish (2.6). For $t \in (0,\tau]$, differentiating the equation in (2.2)

twice with respect to x and setting $\boldsymbol{z} = \partial_x^{\kappa}\boldsymbol{v}, \kappa = 2$, we get

$$\begin{aligned}|\boldsymbol{L}\boldsymbol{z}(x,t)| &= \left|\partial_x^{\kappa}\boldsymbol{f}(x,t) - \sum_{l=0}^{\kappa-1}\binom{\kappa}{l}\boldsymbol{A}_x^{\kappa-l}\partial_x^{l}\boldsymbol{v}(x,t) - \sum_{l=0}^{\kappa}\binom{\kappa}{l}\boldsymbol{B}_x^{\kappa-l}\partial_x^{l}\boldsymbol{v}(x,t-\tau)\right|, \\ &\leq (1+\|\partial_x\boldsymbol{v}\|_{\overline{\Omega}_1})\boldsymbol{C}.\end{aligned} \tag{2.7}$$

Further, since problem (2.4) is independent of the perturbation parameters, it holds $|\boldsymbol{z}(x,0)| \leq \boldsymbol{C}$ in $\overline{D}$, $|\boldsymbol{z}(x,t)| \leq \boldsymbol{C}$ for $(x,t) \in \{0,1\}\times(0,\tau]$. Then using the comparison principle for $\boldsymbol{L}$ with the barrier function $\boldsymbol{\varphi} = \boldsymbol{C}(1+\|\partial_x\boldsymbol{v}\|)t$, we get

$$\left\|\partial_x^2\boldsymbol{v}\right\|_{\overline{\Omega}_1} \leq \boldsymbol{C}_*(1+\|\partial_x\boldsymbol{v}\|_{\overline{\Omega}_1}). \tag{2.8}$$

Further, by using the argument in [109, Lemma 3] and the mean value theorem, we obtain

$$\|\partial_x\boldsymbol{v}\|_{\overline{\Omega}_1} \leq \boldsymbol{C} + \left\|\partial_x^2\boldsymbol{v}\right\|_{\overline{\Omega}_1}/2\boldsymbol{C}_*. \tag{2.9}$$

From (2.8) and (2.9), we get

$$\|\partial_x^s v_\ell\|_{\overline{\Omega}_1} \leq C \quad \text{for} \quad s = 1,2 \quad \ell = 1,2.$$

Next, before establishing bounds on $\|\partial_x^s v_\ell\|_{\overline{\Omega}_1}$, for $s = 3,4$, $\ell = 1,2$, we need to derive bounds on $\left\|\partial_{x,t}^{1,1}\boldsymbol{v}\right\|_{\overline{\Omega}_1}$ and $\left\|\partial_{x,t}^{2,1}\boldsymbol{v}\right\|_{\overline{\Omega}_1}$. For this, we differentiate (2.2) twice and once with respect to x and t, respectively, and define $\tilde{\boldsymbol{z}} = \partial_{x,t}^{\kappa,1}\boldsymbol{v}, \kappa = 2$, to get

$$\begin{aligned}\boldsymbol{L}\tilde{\boldsymbol{z}}(x,t) = \partial_{x,t}^{\kappa,1}\boldsymbol{f}(x,t) &- \sum_{l=0}^{\kappa}\binom{\kappa}{l}\boldsymbol{A}_{x,t}^{\kappa-l,1}\partial_x^{l}\boldsymbol{v}(x,t) - \sum_{l=0}^{\kappa-1}\binom{\kappa}{l}\boldsymbol{A}_x^{\kappa-l}\partial_{x,t}^{l,1}\boldsymbol{v}(x,t) \\ &- \sum_{l=0}^{\kappa}\binom{\kappa}{l}\boldsymbol{B}_{x,t}^{\kappa-l,1}\partial_x^{l}\boldsymbol{v}(x,t-\tau) - \sum_{l=0}^{\kappa}\binom{\kappa}{l}\boldsymbol{B}_x^{\kappa-l}\partial_{x,t}^{l,1}\boldsymbol{v}(x,t-\tau),\end{aligned}$$

and hence

$$|\boldsymbol{L}\tilde{\boldsymbol{z}}(x,t)| \leq (1+\left\|\partial_{x,t}^{1,1}\boldsymbol{v}\right\|_{\overline{\Omega}_1})\boldsymbol{C}.$$

Again using the fact that problem (2.4) is independent of the perturbation parameters, it holds $|\tilde{\boldsymbol{z}}(x,0)| \leq \boldsymbol{C}$ in $\overline{D}$, $|\tilde{\boldsymbol{z}}(x,t)| \leq \boldsymbol{C}$ for $(x,t) \in \{0,1\}\times(0,\tau]$. On applying the comparison principle together with the barrier function $\boldsymbol{\varphi}_1 = \boldsymbol{C}t(1+\left\|\partial_{x,t}^{1,1}\boldsymbol{v}\right\|_{\overline{\Omega}_1})$ gives $\left\|\partial_{x,t}^{2,1}\boldsymbol{v}\right\|_{\overline{\Omega}_1} \leq C_*(1+\left\|\partial_{x,t}^{1,1}\boldsymbol{v}\right\|_{\overline{\Omega}_1})$. Again using the mean value theorem we get

$$\left\|\partial_{x,t}^{1,1}\boldsymbol{v}\right\|_{\overline{\Omega}_1} \leq C + \left\|\partial_{x,t}^{2,1}\boldsymbol{v}\right\|_{\overline{\Omega}_1}/2C_* \tag{2.10}$$

Thus, we have $\left\|\partial_{x,t}^{1,1}\boldsymbol{v}\right\|_{\overline{\Omega}_1} \leq C$ and $\left\|\partial_{x,t}^{2,1}\boldsymbol{v}\right\|_{\overline{\Omega}_1} \leq C$.

Now from the $\ell^{th}, \ell = 1,2$, equation of system (2.7) for $\kappa = 2$, with previously obtained bounds, we get $\|\partial_x^4 v_\ell\|_{\overline{\Omega}_1} \leq c\varepsilon_\ell^{-1}$. Now we apply the argument in [110] to obtain $\|\partial_x^3 v_\ell\|_{\overline{\Omega}_1} \leq c\varepsilon_\ell^{-1/2}$. For $t \in (\tau, 2\tau]$, taking the delay term to the right-hand side, the right-hand side of (2.2) becomes $\boldsymbol{f}(x,t) - \boldsymbol{B}\boldsymbol{v}(x,t-\tau)$, and hence we can use the previous arguments to get $\|\partial_x^s v_\ell\|_{\overline{\Omega}_2} \leq C(1+\varepsilon_\ell^{1-s/2})$, for $s = 1,2,3,4,\ \ell = 1,2$. The proof is completed by using mathematical induction. □

Before we continue further, we define $\mathcal{B}_{\varepsilon_\ell}(x) = e^{-x\sqrt{\alpha/\varepsilon_\ell}} + e^{-(1-x)\sqrt{\alpha/\varepsilon_\ell}},\ \ell = 1,2,\ x \in \overline{\Omega}$. In the following lemma, we derive bounds on the singular part and its derivatives.

Lemma 2.5. *The solution $\boldsymbol{w}$ of problem (2.3) satisfies*

$$|\partial_x^\kappa w_\ell(x,t)| \leq \begin{cases} C\mathcal{B}_{\varepsilon_2}(x), & \kappa = 0, \ell = 1,2, \\ C(\varepsilon_1^{-\kappa/2}\mathcal{B}_{\varepsilon_1}(x) + \varepsilon_2^{-\kappa/2}\mathcal{B}_{\varepsilon_2}(x)), & \kappa = 1,2,3,4, \ell = 1, \\ C\varepsilon_2^{-\kappa/2}\mathcal{B}_{\varepsilon_2}(x), & \kappa = 1,2, \ell = 2 \\ C\varepsilon_2^{-1}(\varepsilon_1^{-(\kappa-2)/2}\mathcal{B}_{\varepsilon_1}(x) + \varepsilon_2^{-(\kappa-2)/2}\mathcal{B}_{\varepsilon_2}(x)), & \kappa = 3,4, \ell = 2, \end{cases} \tag{2.11}$$

for all $(x,t) \in \overline{\Omega}$. *Further, the solution* $\boldsymbol{w} = (w_1, w_2)^T$ *of problem (2.3) can be expressed as* $w_\ell = \widehat{w}_{\ell,\varepsilon_1} + \widehat{w}_{\ell,\varepsilon_2}$ *and* $w_\ell = \tilde{w}_{\ell,\varepsilon_1} + \tilde{w}_{\ell,\varepsilon_2}$, $\ell = 1, 2$, *where*

$$|\partial_x^2 \widehat{w}_{\ell,\varepsilon_1}(x,t)| \leq \varepsilon_\ell^{-1} \mathcal{B}_{\varepsilon_1}(x), \quad |\partial_x^3 \widehat{w}_{\ell,\varepsilon_2}(x,t)| \leq \varepsilon_2^{-3/2} \mathcal{B}_{\varepsilon_2}(x), \tag{2.12}$$

$$|\partial_x^2 \tilde{w}_{\ell,\varepsilon_1}(x,t)| \leq \varepsilon_\ell^{-1} \mathcal{B}_{\varepsilon_1}(x), \quad |\partial_x^4 \tilde{w}_{\ell,\varepsilon_2}(x,t)| \leq \varepsilon_2^{-2} \mathcal{B}_{\varepsilon_2}(x), \tag{2.13}$$

for all $(x,t) \in \overline{\Omega}$.

Proof. The proof of (2.11) can be done using the barrier function approach and the method of steps. It can be done similar to [109]. The proof of (2.12)-(2.13) utilizes (2.11) and can be done similar to [109]. □

Lemma 2.6. *The solution* $\boldsymbol{w}$ *of problem (2.3) satisfies*

$$|\partial_t^s w_\ell(x,t)| \leq C \mathcal{B}_{\varepsilon_2}(x), \quad \textit{for } s = 0, 1, 2, \ \ell = 1, 2, (x,t) \in \overline{\Omega}.$$

Proof. For $t \in (0, \tau]$, note that $|\boldsymbol{w}(x,t)| \leq |\boldsymbol{u}(x,t)| + |\boldsymbol{v}(x,t)| \leq \max_{t\in[0,\tau]}\{|\mathbf{g}_\ell(t)|, |\mathbf{g}_r(t)|\} + \boldsymbol{C} \leq \boldsymbol{C}$ for $x \in \{0,1\}$, and $|\boldsymbol{w}(x,0)| \leq \boldsymbol{C}, x \in \overline{D}$, using (2.3). Thus, for $s = 0$, the result is proved with the barrier function $\boldsymbol{\varphi}_2 = \boldsymbol{C} e^{2\alpha t} \mathcal{B}_{\varepsilon_2}(x)$. To use mathematical induction here, suppose that the result of this lemma holds for $s = 0, \ldots, m-1$, $1 \leq m \leq 2$. Now we will derive a bound for $s = m$. Define $\tilde{\mathbf{g}} = \partial_t^m \boldsymbol{w}$, we have

$$\begin{cases} \boldsymbol{L}\tilde{\mathbf{g}}(x,t) := \partial_t \tilde{\mathbf{g}}(x,t) - \boldsymbol{E}\partial_x^2 \tilde{\mathbf{g}}(x,t) + \boldsymbol{A}\tilde{\mathbf{g}}(x,t) \\ \qquad\qquad = -\sum_{l=0}^{m-1} \binom{m}{l} \boldsymbol{A}_t^{(m-l)} \partial_t^l \boldsymbol{w}(x,t) - \sum_{l=0}^{m} \binom{m}{l} \boldsymbol{B}_t^{(m-l)} \partial_t^l \boldsymbol{w}(x,t-\tau) \\ \qquad\qquad := \tilde{\mathbf{g}}_m \ \text{ in } \Omega_1 = (0,1) \times (0,\tau], \end{cases}$$

and

$$\begin{cases} |\tilde{\mathbf{g}}(x,0)| \leq \boldsymbol{C} \ \text{ in } \overline{D}, \\ |\tilde{\mathbf{g}}(x,t)| \leq \max\{|\mathbf{g}_\ell^m(t)|, |\mathbf{g}_r^m(t)|\} + |\partial_t^m \boldsymbol{v}| \leq \boldsymbol{C} \ \text{ for } (x,t) \in \{0,1\} \times (0,\tau], \end{cases}$$

where bounds on the boundary conditions follow from (2.3). Using mathematical induction, we get $|\tilde{\mathbf{g}}_m(x,t)| \leq \boldsymbol{L}\boldsymbol{\varphi}_2(x,t)$. Hence, using the maximum principle for the operator $\boldsymbol{L}$ with the barrier function $\boldsymbol{\varphi}_2$ we get the required result for $t \in (0,\tau]$. For $t \in (\tau, 2\tau]$, we apply the previous arguments to get $|\partial_t^s w_\ell(x,t)| \leq C\mathcal{B}_{\varepsilon_2}(x)$, for $s = 0,1,2,\ \ell = 1,2$. The result is completed using mathematical induction. □

2.2 Splitting schemes based fitted mesh method

From the asymptotic behavior described in the above lemmas, it follows that the solution has overlapping layers at $x = 0$ and $x = 1$. Thus, the domain Ω is discretized as $\overline{\Omega}^{N,M} = \overline{D}^N \times \overline{\omega}^M$, where $\overline{D}^N = \{x_i\}_{i=0}^N$ denotes the space discretization using a layer adapted mesh and $\overline{\omega}^M = \{t_j\}_{j=0}^M$ denotes the time discretization using a uniform mesh. We define $\Omega^{N,M} = \overline{\Omega}^{N,M} \cap \Omega; \mathbf{\Gamma}^{N,M} = \overline{\Omega}^{N,M} \setminus \Omega^{N,M}; \mathbf{\Gamma}_\gamma^{N,M} = \mathbf{\Gamma}^{N,M} \cap \mathbf{\Gamma}_\gamma, \gamma = \ell, r$. Also, $\overline{\Omega}_p^{N,m_\tau} = \overline{D}^N \times \overline{\omega}_p^{m_\tau}$, where $\overline{\omega}_p^{m_\tau} = \{t_j : (p-1)\tau = t_{pm_\tau} < t_{pm_\tau+1} < \cdots < t_{pm_\tau+m_\tau-1} < t_{(p+1)m_\tau} = p\tau\}$; $\Omega_p^{N,m_\tau} = \overline{\Omega}_p^{N,m_\tau} \cap \Omega_p$, where $\Omega_p = D \times ((p-1)\tau,\ p\tau]$; $\mathbf{\Gamma}_p^{N,m_\tau} = \overline{\Omega}_p^{N,m_\tau} \setminus \Omega_p^{N,m_\tau}; \mathbf{\Gamma}_{p,\gamma}^{N,m_\tau} = \mathbf{\Gamma}_p^{N,m_\tau} \cap \mathbf{\Gamma}_\gamma, p = 0,\ldots,n, \gamma = \ell, r$. Further, the mesh spacing in space and time directions are defined as $h_i = x_i - x_{i-1},\ i = 1,\ldots,N$, and $\Delta t = T/M$ with $M = nm_\tau$, where m_τ denotes the number of subintervals on each $[(p-1)\tau, p\tau]$. The following two layer adapted meshes are used in the spatial direction.

Shishkin mesh [109]: The space domain $[0,1]$ is partitioned into five subdomains $D_1 = [0,\rho_1],\ D_2 = [\rho_1,\rho_2],\ D_3 = [\rho_2, 1-\rho_2],\ D_4 = [1-\rho_2, 1-\rho_1]$ and $D_5 = [1-\rho_1, 1]$

such that $\overline{D} = \cup_{i=1}^{5} D_i$. On each subdomain $D_q,\ q = 1, 2, 4, 5$, a uniform mesh with $N/8+1$ mesh points is placed and on the subdomain D_3 a uniform mesh with $N/2+1$ mesh points is placed. The transition parameters are taken as follows

$$\rho_2 = \min\left\{\frac{1}{4}, 2\sqrt{\frac{\varepsilon_2}{\alpha}}\ln N\right\}, \quad \rho_1 = \min\left\{\frac{\rho_2}{2}, 2\sqrt{\frac{\varepsilon_1}{\alpha}}\ln N\right\}.$$

In our analysis, for simplicity, we will consider the most interesting case $\rho_2 = 2\sqrt{\frac{\varepsilon_2}{\alpha}}\ln N$ and $\rho_1 = 2\sqrt{\frac{\varepsilon_1}{\alpha}}\ln N$.

Generalized Shishkin mesh [111]: This mesh also uses two transition parameters $\rho_2 = \min\left\{\frac{1}{4}, 2\sqrt{\frac{\varepsilon_2}{\alpha}}\lambda\right\},\ \rho_1 = \min\left\{\frac{\rho_2}{2}, 2\sqrt{\frac{\varepsilon_1}{\alpha}}\lambda\right\}$, where $\lambda = \lambda(N)$ satisfies $\ln(\ln N) \leq \lambda \leq \ln N$ and $e^{-\lambda} \leq \lambda/N$. Let $N = 8k$, where k is a positive integer. Then, the mesh points are defined as

$$x_i = \begin{cases} \psi(i/N), & \text{for } i \leq N/2, \\ 1 - \psi((N-i)/N), & \text{for } i > N/2. \end{cases} \tag{2.14}$$

For $\rho_2 = 1/4$ and $\rho_1 = 1/8$ the mesh will be uniform; we consider $\rho_1 = 2\sqrt{\frac{\varepsilon_1}{\alpha}}\lambda$ which is the most interesting case in practice. For $\rho_2 \neq 1/4$, the mesh generating function $\psi \in C^1[0, 1/2]$ is given by

$$\psi(\zeta) = \begin{cases} 8\zeta\rho_1, & \zeta \in [0, \frac{1}{8}], \\ 8^3(\rho_2 - 2\rho_1)(\zeta - \frac{1}{8})^3 + 8\rho_1(\zeta - \frac{1}{8}) + \rho_1, & \zeta \in [\frac{1}{8}, \frac{1}{4}], \\ 64(\frac{1}{2} - 7\rho_2 + 10\rho_1)(\zeta - \frac{1}{4})^3 + (24\rho_2 - 40\rho_1)(\zeta - \frac{1}{4}) + \rho_2, & \zeta \in [\frac{1}{4}, \frac{1}{2}]. \end{cases}$$

We assume that $\psi'(\zeta) \geq 0$ that $\psi''(\zeta) \geq 0$, so that $\psi(\zeta)$ is increasing function and $h_i \geq h_{i-1},\ i = 2, \ldots, N/2$. Thus, the condition $1/2 - 7\rho_2 + 10\rho_1 \geq 0$ must be satisfied. Note that this mesh is uniform on $[0, \rho_1]$ and $[1-\rho_1, 1]$, and nonuniform on $[\rho_1, \rho_2]$, $[\rho_2, 1-\rho_2]$ and $[1-\rho_2, 1-\rho_1]$. Further, following [111] we have $h_\gamma \leq CN^{-1}, \gamma =$

$1, \ldots, N$, and

$$|h_{\gamma+1} - h_\gamma| = \begin{cases} C\varepsilon_2^{1/2} N^{-2}\lambda, & N/8 \le \gamma \le N/4 - 1, \\ CN^{-2}, & N/4 \le \gamma \le N/2 - 1. \end{cases}$$

Otherwise, if $\rho_2 = 1/4$ or $1/2 - 7\rho_2 + 10\rho_1 < 0$, the mesh is defined by

$$x_i = \begin{cases} \tilde{\psi}(i/N), & \text{for } i \le N/2, \\ 1 - \tilde{\psi}((N-i)/N), & \text{for } i > N/2, \end{cases} \tag{2.15}$$

with $\tilde{\psi} \in C^2[0,1]$ and

$$\tilde{\psi}(\zeta) = \begin{cases} 8\zeta\rho_1, & \zeta \in [0, \frac{1}{8}], \\ (8/3)^3(\frac{1}{2} - 4\rho_1)(\zeta - \frac{1}{8})^3 + 8\rho_1(\zeta - \frac{1}{8}) + \rho_1, & \zeta \in [\frac{1}{8}, \frac{1}{2}]. \end{cases}$$

Here the mesh spacing satisfy $|\tilde{h}_{\gamma+1} - \tilde{h}_\gamma| \le CN^{-2}$ for $\gamma = N/8, \ldots, N/2 - 1$.

On the domain $\overline{\Omega}^{N,M}$, we discretize problem (2.1) by

$$\boldsymbol{L}^{N,M}\mathbf{U}(x_i, t_j) + \boldsymbol{B}_{i,j}\mathbf{U}(x_i, t_{j-m_\tau}) = \boldsymbol{f}(x_i, t_j), \quad (x_i, t_j) \in \Omega^{N,M}, \tag{2.16}$$

with

$$\begin{cases} \mathbf{U}(x_i, t_j) = \mathbf{g}_b(x_i, t_j) & \text{for } (x_i, t_j) \in \overline{\Omega}_0^{N,m_\tau}, \\ \mathbf{U}(x_0, t_j) = \mathbf{g}_\ell(t_j), \mathbf{U}(x_N, t_j) = \mathbf{g}_r(t_j) & \text{for } t_j \in \overline{\omega}^M, \end{cases} \tag{2.17}$$

where

$$\boldsymbol{L}^{N,M}\mathbf{U}(x_i, t_j) = (\delta_t\mathbf{U} - \boldsymbol{\mathcal{E}}\delta_x^2\mathbf{U} + \boldsymbol{P}_{i,j}\mathbf{U})(x_i, t_j) - \boldsymbol{S}_{i,j}\mathbf{U}(x_i, t_{j-1}),$$

$$\delta_x^2\mathbf{Y}_{i,j} = \frac{2}{h_i + h_{i+1}}\left(\frac{\mathbf{Y}_{i+1,j} - \mathbf{Y}_{i,j}}{h_{i+1}} - \frac{\mathbf{Y}_{i,j} - \mathbf{Y}_{i-1,j}}{h_i}\right), \quad \delta_t\mathbf{Y}_{i,j} = \frac{\mathbf{Y}_{i,j} - \mathbf{Y}_{i,j-1}}{\Delta t},$$

and $\boldsymbol{A}_{i,j} = \boldsymbol{P}_{i,j} - \boldsymbol{S}_{i,j}$. Note that if $\boldsymbol{P}_{i,j} = \boldsymbol{A}_{i,j}$, the time discretization uses the classical implicit scheme which is considered in [52]. Here, in order to decouple the components of the solution, we consider $\boldsymbol{P}_{i,j}$ as follows [107]

$$\boldsymbol{P}_{i,j} \in \{diag(\boldsymbol{A}_{i,j}),\ ltr(\boldsymbol{A}_{i,j})\}\,,$$

$$diag(\boldsymbol{A}_{i,j}) = \begin{pmatrix} a_{11}(x_i,t_j) & 0 \\ 0 & a_{22}(x_i,t_j) \end{pmatrix},\ ltr(\boldsymbol{A}_{i,j}) = \begin{pmatrix} a_{11}(x_i,t_j) & 0 \\ a_{21}(x_i,t_j) & a_{22}(x_i,t_j) \end{pmatrix}.$$

So, we have two choices for $\boldsymbol{P}_{i,j}$. Then, we use $\boldsymbol{A}_{i,j} = \boldsymbol{P}_{i,j} - \boldsymbol{S}_{i,j}$ to find $\boldsymbol{S}_{i,j}$ accordingly. Both the choices decouple the system, and hence, resulted in a reduced computational time.

2.3 Convergence analysis

In this section, we analyze the uniform convergence of the scheme (2.16)-(2.17) on the rectangular meshes $\overline{\Omega}^{N,M}$ generated using Shishkin mesh and generalized Shishkin mesh (2.14) in space and a uniform mesh in time. The uniform convergence analysis on the rectangular mesh $\overline{\Omega}^{N,M}$ generated using generalized Shishkin mesh (2.15) in space can be done in similar way. We first introduce the maximum principle for the discrete operator and then establish the theorem concerning the convergence analysis.

Lemma 2.7. If the mesh function $\boldsymbol{\phi}$ satisfies $\boldsymbol{\phi}(x_i,t_j) \geq \mathbf{0}$ for $(x_i,t_j) \in \boldsymbol{\Gamma}^{N,M}$, and discrete operator $\boldsymbol{L}^{N,M}$ satisfies $\boldsymbol{L}^{N,M}\boldsymbol{\phi}(x_i,t_j) \geq \mathbf{0}$ for $(x_i,t_j) \in \Omega^{N,M}$. Then $\boldsymbol{\phi}(x_i,t_j) \geq \mathbf{0}$ for $(x,t) \in \overline{\Omega}^{N,M}$.

Proof. The proof follows using the arguments in ([108]). □

Theorem 2.8. The uniform error estimate associated to the scheme (2.16)-(2.17) *satisfies*

$$||\boldsymbol{u}-\mathbf{U}||_{\overline{\Omega}^{N,M}} \leq C \begin{cases} \Delta t + N^{-2}\ln^2 N & \text{for Shishkin mesh,} \\ \Delta t + N^{-2}\lambda^2 & \text{for generalized Shishkin mesh.} \end{cases} \tag{2.18}$$

Proof. Taking $(x_i,t_j) \in \overline{\Omega}_1^{N,m_\tau}$ and $\boldsymbol{P}_{i,j} = \left\{ \begin{pmatrix} a_{11}(x_i,t_j) & 0 \\ 0 & a_{22}(x_i,t_j) \end{pmatrix} \right\}$, we have

$$\boldsymbol{L}^{N,M}(\boldsymbol{u}-\mathbf{U})(x_i,t_j) = [\boldsymbol{L}^{N,M}\boldsymbol{u}-\boldsymbol{L}\boldsymbol{u}](x_i,t_j)$$

$$= [\delta_t\boldsymbol{u}-\partial_t\boldsymbol{u}](x_i,t_j) - \boldsymbol{\mathcal{E}}[\delta_x^2\boldsymbol{u}-\partial_x^2\boldsymbol{u}](x_i,t_j) + \boldsymbol{S}_{i,j}[\boldsymbol{u}(x_i,t_j)-\boldsymbol{u}(x_i,t_{j-1})]$$

Define $\boldsymbol{L}^{N,M} = (L_1^{N,M}, L_2^{N,M})^T$. Thus, for $m = 1, 2$, we can write

$$|L_m^{N,M}(u-U)(x_i,t_j)| \leq |\left(\delta_t - \partial_t\right) u_m(x_i,t_j)| + C|(u_{3-m}(x_i,t_j) - u_{3-m}(x_i,t_{j-1}))| + \varepsilon_m \left|\left(\partial_x^2 - \delta_x^2\right) u_m(x_i,t_j)\right|.$$

Using Taylor expansions and bounds in Lemma 2.3, we get

$$|\left(\delta_t - \partial_t\right) u_m(x_i,t_j)| + C|u_{3-m}(x_i,t_j) - u_{3-m}(x_i,t_{j-1})|$$

$$\leq C(t_j - t_{j-1}) \left(\|\partial_t u_{3-m}(x_i,.)\|_{[t_{j-1},t_j]} + \left\|\partial_t^2 u_m(x_i,.)\right\|_{[t_{j-1},t_j]} \right)$$

$$\leq C\Delta t \quad \text{for } (x_i,t_j) \in \Omega_1^{N,m_\tau},\ m = 1,2.$$

Next, we need the bound for $\varepsilon_m|[\partial_x^2 u_m - \delta_x^2 u_m](x_i,t_j)|$. We distinguish two cases depending on the mesh used in the spatial direction. Suppose Shishkin mesh is used in the space. Now, using the arguments in [52] we have

$$\varepsilon_m|[\partial_x^2 u_m - \delta_x^2 u_m](x_i,t_j)| \leq \begin{cases} C(N^{-1}\ln N)^2,\ x_i \neq \rho_1,\rho_2,1-\rho_1,1-\rho_2,\ t_j \in \overline{\omega}_1^{m_\tau}, \\ \qquad\qquad m=1,2, \\ C\frac{\sqrt{\varepsilon_1}}{\sqrt{\varepsilon_2}}N^{-1}+CN^{-2},\ x_i \in \{\rho_1,1-\rho_1\},\ t_j \in \overline{\omega}_1^{m_\tau}, m=1, \\ C\frac{\sqrt{\varepsilon_2}}{\sqrt{\varepsilon_1}}N^{-1}+CN^{-2},\ x_i \in \{\rho_1,1-\rho_1\},\ t_j \in \overline{\omega}_1^{m_\tau}, m=2, \\ C\frac{\varepsilon_1}{\sqrt{\varepsilon_2}}N^{-1}+CN^{-2},\ x_i \in \{\rho_2,1-\rho_2\},\ t_j \in \overline{\omega}_1^{m_\tau}, m=1, \\ C\sqrt{\varepsilon_2}N^{-1}+CN^{-2},\ x_i \in \{\rho_2,1-\rho_2\},\ t_j \in \overline{\omega}_1^{m_\tau}, m=2. \end{cases} \tag{2.19}$$

Otherwise when generalized Shishkin mesh is used, using the arguments in [52] we have

$$\varepsilon_m|[\partial_x^2 u_m - \delta_x^2 u_m](x_i,t_j)| \leq CN^{-2}\lambda^2. \tag{2.20}$$

Next, we define the mesh function

$$\boldsymbol{\psi} := \begin{cases} \hat{\boldsymbol{C}}\Delta t + \hat{\boldsymbol{C}}N^{-2}\ln^2 N(1+\varphi_{\varepsilon_1}+\varphi_{\varepsilon_2}) \pm (\boldsymbol{u}-\mathbf{U}) & \text{for Shishkin mesh,} \\ \hat{\boldsymbol{C}}\Delta t + \hat{\boldsymbol{C}}N^{-2}\lambda^2 \pm (\boldsymbol{u}-\mathbf{U}) & \text{for generalized Shishkin mesh,} \end{cases} \tag{2.21}$$

where $\varphi_{\varepsilon_m},\ m=1,2$, are defined as follows

$$\varphi_{\varepsilon_m}(x,t) = \begin{cases} \frac{x}{\rho_m}, & 0 \leq x \leq \rho_m,\ 0 \leq t \leq \tau \\ 1, & \rho_m \leq x \leq 1-\rho_m,\ 0 \leq t \leq \tau, \\ \frac{1-x}{\rho_m}, & 1-\rho_m \leq x \leq 1.\ 0 \leq t \leq \tau. \end{cases} \tag{2.22}$$

Note that

$$-\delta_x^2(\varphi_{\varepsilon_1})_{i,j} \geq \begin{cases} \frac{\alpha N}{32\sqrt{\varepsilon_1}\sqrt{\varepsilon_2}\ln^2 N}, & \text{if } x_i \in \{\rho_1,1-\rho_1\}, \\ 0, & \text{otherwise} \end{cases}$$

and

$$-\delta_x^2(\varphi_{\varepsilon_2})_{i,j} \geq \begin{cases} \frac{\sqrt{\alpha}N}{2\sqrt{\varepsilon_2}\ln N}, & \text{if } x_i \in \{\rho_2, 1-\rho_2\}, \\ 0, & \text{otherwise.} \end{cases}$$

Clearly,

$$\boldsymbol{\psi}(x_i, t_j) \geq \mathbf{0} \quad \text{for} \quad (x_i, t_j) \in \boldsymbol{\Gamma}_{1,\ell}^{N,m_\tau} \cup \boldsymbol{\Gamma}_{1,r}^{N,m_\tau} \cup \boldsymbol{\Gamma}_b^{N,m_\tau}.$$

Now recalling the truncation error bound we can choose $\hat{\boldsymbol{C}}$ sufficiently large, independent of the perturbation parameters ε_1 and ε_2, so that

$$\boldsymbol{L}^{N,M}\boldsymbol{\psi}(x_i, t_j) \geq \mathbf{0} \quad \text{for } \Omega_1^{N,m_\tau}.$$

Hence, using the discrete maximum principle we get $\boldsymbol{\psi}(x_i, t_j) \geq \mathbf{0}$ for $(x_i, t_j) \in \overline{\Omega}_1^{N,M}$. Consequently

$$||\boldsymbol{u} - \mathbf{U}||_{\overline{\Omega}_1^{N,m_\tau}} \leq C \begin{cases} \Delta t + N^{-2}\ln^2 N & \text{for Shishkin mesh,} \\ \Delta t + N^{-2}\lambda^2 & \text{for generalized Shishkin mesh.} \end{cases} \tag{2.23}$$

Next, for $(x_i, t_j) \in \overline{\Omega}_2^{N,m_\tau}$, we have

$$|\boldsymbol{L}^{N,M}(\boldsymbol{u} - \mathbf{U})(x_i, t_j)| \leq |\boldsymbol{B}_{i,j}(\boldsymbol{u} - \mathbf{U})(x_i, t_{j-m_\tau})| + |(\delta_t \boldsymbol{u} - \partial_t \boldsymbol{u})(x_i, t_j)| +$$

$$\boldsymbol{\mathcal{E}}|(\partial_x^2 \boldsymbol{u} - \delta_x^2 \boldsymbol{u})(x_i, t_j)| + |\boldsymbol{S}_{i,j}(\boldsymbol{u}(x_i, t_j) - \boldsymbol{u}(x_i, t_{j-1}))|.$$

The bound for the first term follows using (2.23) as $(x_i, t_{j-m_\tau}) \in \overline{\Omega}_1^{N,m_\tau}$. Further, using Taylor expansion and Lemma 2.3, we have $|(\delta_t \boldsymbol{u} - \partial_t \boldsymbol{u})(x_i, t_j)| + |\boldsymbol{S}_{i,j}(\boldsymbol{u}(x_i, t_j) - \boldsymbol{u}(x_i, t_{j-1}))| \leq \mathbf{C}\Delta t$. Using previous arguments, we can derive bounds similar to

(2.19)-(2.20) for $\boldsymbol{\mathcal{E}}|(\partial_x^2\boldsymbol{u} - \delta_x^2\boldsymbol{u})(x_i, t_j)|$. Now, applying the discrete maximum principle to the barrier function (2.21)-(2.22) it holds

$$||\boldsymbol{u} - \mathbf{U}||_{\overline{\Omega}_2^{N,m_\tau}} \leq C \begin{cases} \Delta t + N^{-2}\ln^2 N & \text{for Shishkin mesh,} \\ \Delta t + N^{-2}\lambda^2 & \text{for generalized Shishkin mesh.} \end{cases} \tag{2.24}$$

Thus, the final result (2.18) follows using the mathematical induction. Further, we can obtain similar bounds for another choice of $\boldsymbol{P}_{i,j}$ using the above arguments. □

2.4 Numerical results

We perform numerical experiments on two test problems to validate our theoretically proven results of the previous section.

Example 2.1. Consider problem (2.1) with the following data

$$\begin{cases} \boldsymbol{u}(x,t) = \boldsymbol{g}_b(x,t) = \mathbf{0}, & 0 \leq x \leq 1, -1 \leq t \leq 0, \\ \boldsymbol{u}(0,t) = \boldsymbol{g}_\ell(t) = \mathbf{0}, \boldsymbol{u}(1,t) = \boldsymbol{g}_r(t) = \mathbf{0}, & 0 < t \leq 2, \end{cases}$$

where

$$\boldsymbol{A} = \begin{pmatrix} 3(1+x)^2 & -1-x^3 \\ -2\cos(\pi x/4) & 4\exp(1-x) \end{pmatrix}, \ \boldsymbol{B} = \begin{pmatrix} -1 & 0 \\ 0 & -1 \end{pmatrix}, \boldsymbol{f} = \begin{pmatrix} \cos(\pi x/2) \\ x \end{pmatrix}.$$

The maximum pointwise errors $\mathbf{E}_{\varepsilon_1,\varepsilon_2}^{N,\Delta t}$ for this problem are computed using double mesh principle as follows

$$\mathbf{E}_{\varepsilon_1,\varepsilon_2}^{N,\Delta t} = ||\mathbf{U}^{N,\Delta t} - \mathbf{U}^{2N,\Delta t/4}||_{\overline{\Omega}^{N,M}}$$

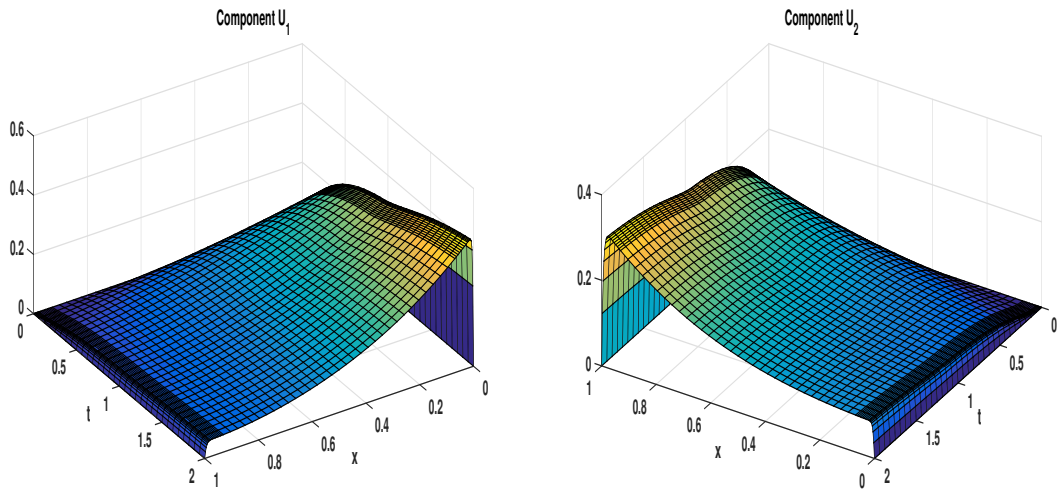

FIGURE 2.1: Solution profile with $\boldsymbol{P}_{i,j} = diag(\boldsymbol{A}_{i,j})$ for Example 2.1 using Shishkin mesh for $\varepsilon_1 = 10^{-5}, \varepsilon_2 = 10^{-4}$ with $N = 64, M = 32$.

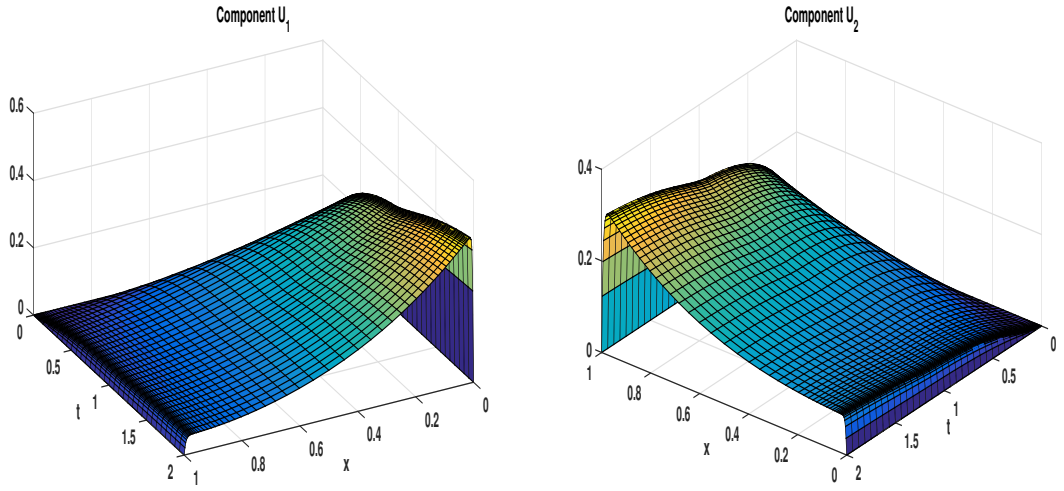

FIGURE 2.2: Solution profile with $\boldsymbol{P}_{i,j} = diag(\boldsymbol{A}_{i,j})$ for Example 2.1 using generalized Shishkin mesh for $\varepsilon_1 = 10^{-5}, \varepsilon_2 = 10^{-4}$ with $N = 64, M = 32$.

where the solution $\mathbf{U}^{N,\Delta t}$ is obtained on the layer adapted mesh with $N+1$ mesh points in space and Δt step length in time direction, and $\mathbf{U}^{2N,\Delta t/4}$ is computed on the layer adapted mesh with $2N+1$ mesh points in space and $\Delta t/4$ step length in time direction but with the same values of transition parameters as for $\mathbf{U}^{N,\Delta t}$.

The solution plots are given in Figures 2.1 and 2.2 showing the boundary layers

TABLE 2.1: Uniform errors $\mathbf{E}^{N,\Delta t}$ and uniform convergence rates $\mathbf{R}^{N,\Delta t}$ using Shishkin mesh for Example 2.1.

Schemes		$N=32$ $\Delta t=1/4$	$N=64$ $\Delta t=1/4^2$	$N=128$ $\Delta t=1/4^3$	$N=256$ $\Delta t=1/4^4$	$N=512$ $\Delta t=1/4^5$
$\boldsymbol{P}_{i,j}=diag(\boldsymbol{A}_{i,j})$	$E_1^{N,\Delta t}$	8.0703e-02	5.5478e-02	2.7588e-02	9.5568e-03	2.4838e-03
	$R_1^{N,\Delta t}$	0.540	1.007	1.529	1.944	
	$E_2^{N,\Delta t}$	2.7366e-02	1.3156e-02	5.5693e-03	2.0507e-03	7.3946e-04
	$R_2^{N,\Delta t}$	1.056	1.240	1.441	1.471	
$\boldsymbol{P}_{i,j}=ltr(\boldsymbol{A}_{i,j})$	$E_1^{N,\Delta t}$	7.4751e-02	5.2969e-02	2.6753e-02	9.3441e-03	2.4384e-03
	$R_1^{N,\Delta t}$	0.496	9.854	1.517	1.938	
	$E_2^{N,\Delta t}$	2.5404e-02	1.3047e-02	5.5491e-03	2.0525e-03	7.3969e-04
	$R_2^{N,\Delta t}$	0.961	1.233	1.434	1.472	
$\boldsymbol{P}_{i,j}=\boldsymbol{A}_{i,j}$	$E_1^{N,\Delta t}$	7.9563e-02	5.5220e-02	2.7527e-02	9.5459e-03	2.4822e-03
	$R_1^{N,\Delta t}$	0.526	1.004	1.527	1.943	
	$E_2^{N,\Delta t}$	3.4391e-02	1.6963e-02	5.9513e-03	2.0574e-03	7.0051e-04
	$R_2^{N,\Delta t}$	1.019	1.511	1.532	1.554	

TABLE 2.2: Uniform errors $\mathbf{E}^{N,\Delta t}$ and uniform convergence rates $\mathbf{R}^{N,\Delta t}$ using generalized Shishkin mesh for Example 2.1.

Schemes		$N=32$ $\Delta t=1/4$	$N=64$ $\Delta t=1/4^2$	$N=128$ $\Delta t=1/4^3$	$N=256$ $\Delta t=1/4^4$	$N=512$ $\Delta t=1/4^5$
$\boldsymbol{P}_{i,j}=diag(\boldsymbol{A}_{i,j})$	$E_1^{N,\Delta t}$	8.0703e-02	5.5478e-02	2.7588e-02	9.5568e-03	2.4838e-03
	$R_1^{N,\Delta t}$	0.540	1.007	1.529	1.944	
	$E_2^{N,\Delta t}$	2.6458e-02	1.0421e-02	3.2445e-03	9.3228e-04	2.6066e-04
	$R_2^{N,\Delta t}$	1.344	1.683	1.799	1.838	
$\boldsymbol{P}_{i,j}=ltr(\boldsymbol{A}_{i,j})$	$E_1^{N,\Delta t}$	7.4751e-02	5.2969e-02	2.6753e-02	9.3441e-03	2.4384e-03
	$R_1^{N,\Delta t}$	0.496	0.985	1.517	1.938	
	$E_2^{N,\Delta t}$	2.5404e-02	9.3939e-03	3.0725e-03	8.9322e-04	2.5237e-04
	$R_2^{N,\Delta t}$	1.435	1.612	1.782	1.823	
$\boldsymbol{P}_{i,j}=\boldsymbol{A}_{i,j}$	$E_1^{N,\Delta t}$	7.9563e-02	5.5220e-02	2.7527e-02	9.5459e-03	2.9737e-03
	$R_1^{N,\Delta t}$	0.526	1.004	1.527	1.710	
	$E_2^{N,\Delta t}$	3.4391e-02	1.6963e-02	5.9513e-03	1.9340e-03	6.0213e-04
	$R_2^{N,\Delta t}$	1.019	1.511	1.622	1.683	

at $x=0$ and $x=1$. In Tables 2.1 and 2.2 we report the componentwise uniform errors $\mathbf{E}^{N,\Delta t}$ with corresponding uniform convergence rates $\mathbf{R}^{N,\Delta t}$ which are computed using the three choices of $\boldsymbol{P}_{i,j}$ on Shishkin and generalized Shishkin meshes, respectively, for Example 2.1.

Example 2.2. Consider problem (2.1) with the following data

$$\begin{cases} \boldsymbol{u}(x,t)=\boldsymbol{g}_b(x,t), & 0\le x\le 1,-1\le t\le 0,\\ \boldsymbol{u}(0,t)=\boldsymbol{g}_\ell(t),\ \boldsymbol{u}(1,t)=\boldsymbol{g}_r(t), & 0<t\le 2, \end{cases}$$

with

$$\boldsymbol{A} = \begin{pmatrix} 3 & -1 \\ -1 & 3 \end{pmatrix}, \ \boldsymbol{B} = \begin{pmatrix} -1 & 0 \\ 0 & -1 \end{pmatrix},$$

where $\boldsymbol{f} = (f_1, f_2)^T, \mathbf{g}_b, \mathbf{g}_\ell$ and $\mathbf{g}_r$ are determined taking components of the exact solution as follows

$$u_1(x,t) = t(\eta_1(x) + \eta_2(x) - 2) + t(1+x)e^{-t},$$

$$u_2(x,t) = \varepsilon_1(\eta_1(x) - 1)(1 - e^{-t}) + t(\eta_2(x) - 1)(1-t),$$

with

$$\eta_j(x) = \frac{\exp\left(-x/\sqrt{\varepsilon_j}\right) + \exp\left(-(1-x)/\sqrt{\varepsilon_j}\right)}{1 + \exp\left(-1/\sqrt{\varepsilon_j}\right)}, \quad j = 1, 2.$$

Since the exact solution is available, the maximum pointwise errors for this problem are calculated as $\mathbf{E}^{N,\Delta t}_{\varepsilon_1,\varepsilon_2} = ||\boldsymbol{u} - \mathbf{U}^{N,\Delta t}||_{\overline{\Omega}^{N,M}}$. The uniform errors $\mathbf{E}^{N,\Delta t}$ for both the problems are calculated as follows

$$\mathbf{E}^{N,\Delta t} = \max_{\varepsilon_1} \mathbf{E}^{N,\Delta t}_{\varepsilon_1}$$

where $\mathbf{E}^{N,\Delta t}_{\varepsilon_1} = \max\{\mathbf{E}^{N,\Delta t}_{\varepsilon_1,1}, \mathbf{E}^{N,\Delta t}_{\varepsilon_1,10^{-1}}, \ldots, \mathbf{E}^{N,\Delta t}_{\varepsilon_1,10^{-k}}\}$ is calculated for a fixed $\varepsilon_1 = 10^{-k}$, k is a non-negative integer. Further, we define the uniform rates of convergence as follows

$$\mathbf{R}^{N,\Delta t} = \log_2(\mathbf{E}^{N,\Delta t}/\mathbf{E}^{2N,\Delta t/4}).$$

Tables 2.3 and 2.4 display the componentwise uniform errors $\mathbf{E}^{N,\Delta t}$ with corresponding convergence rates $\mathbf{R}^{N,\Delta t}$ for Example 2.2. The reported results show that the uniform errors have similar behavior for the splitting schemes and the classical scheme $\boldsymbol{P}_{i,j} = \boldsymbol{A}_{i,j}$. Further, second order uniform convergence in space is clearly seen from these tables. In order to show the convergence in time, we display uniform errors

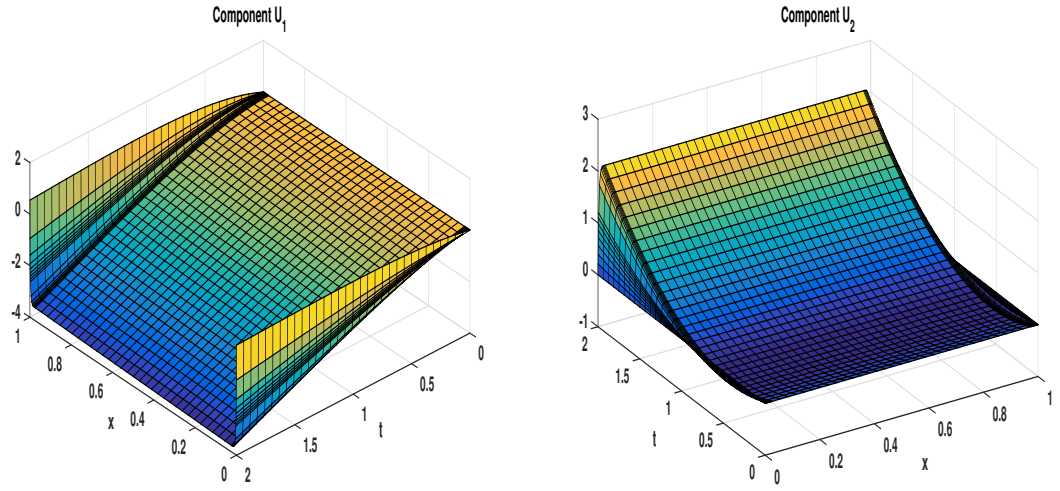

FIGURE 2.3: Solution profile with $\boldsymbol{P}_{i,j} = diag(\boldsymbol{A}_{i,j})$ for Example 2.2 using Shishkin mesh for $\varepsilon_1 = 10^{-7}, \varepsilon_2 = 10^{-5}$ with $N = 64, M = 32$.

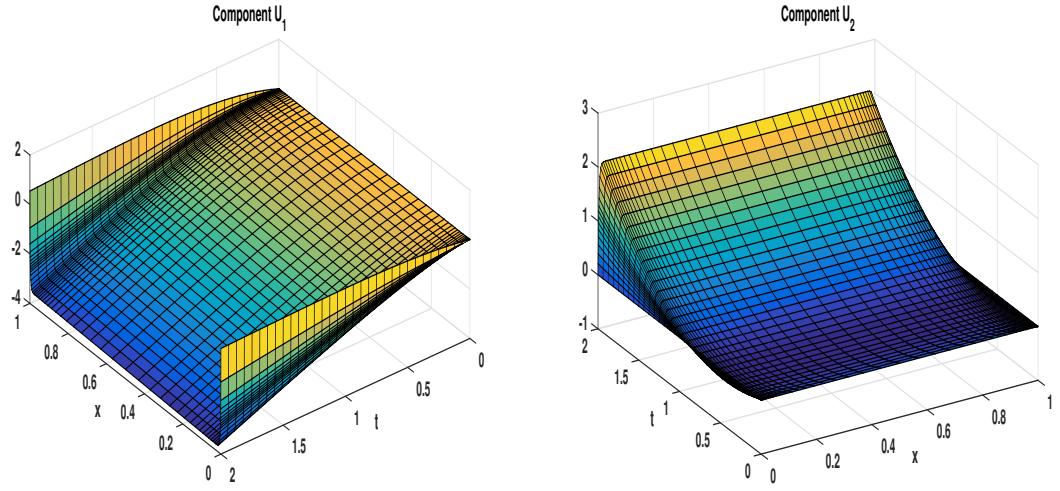

FIGURE 2.4: Solution profile with $\boldsymbol{P}_{i,j} = diag(\boldsymbol{A}_{i,j})$ for Example 2.2 using generalized Shishkin mesh for $\varepsilon_1 = 10^{-7}, \varepsilon_2 = 10^{-5}$ with $N = 64, M = 32$.

TABLE 2.3: Uniform errors $\mathbf{E}^{N,\Delta t}$ and uniform convergence rates $\mathbf{R}^{N,\Delta t}$ using Shishkin mesh for Example 2.2.

Schemes		$N=32$ $\Delta t=1/4$	$N=64$ $\Delta t=1/4^2$	$N=128$ $\Delta t=1/4^3$	$N=256$ $\Delta t=1/4^4$	$N=512$ $\Delta t=1/4^5$
$\boldsymbol{P}_{i,j}=diag(\boldsymbol{A}_{i,j})$	$E_1^{N,\Delta t}$	2.2797e-01	1.6056e-01	7.4906e-02	2.4873e-02	6.3341e-03
	$R_1^{N,\Delta t}$	0.505	1.100	1.590	1.973	
	$E_2^{N,\Delta t}$	2.9156e-01	7.3930e-02	2.0584e-02	5.6177e-03	1.6360e-03
	$R_2^{N,\Delta t}$	1.979	1.844	1.873	1.779	
$\boldsymbol{P}_{i,j}=ltr(\boldsymbol{A}_{i,j})$	$E_1^{N,\Delta t}$	2.2783e-01	1.6049e-01	7.4881e-02	2.4866e-02	6.3324e-03
	$R_1^{N,\Delta t}$	0.505	1.099	1.590	1.973	
	$E_2^{N,\Delta t}$	2.9124e-01	7.3833e-02	2.0584e-02	5.6175e-03	1.3635e-03
	$R_2^{N,\Delta t}$	1.979	1.842	1.873	2.042	
$\boldsymbol{P}_{i,j}=\boldsymbol{A}_{i,j}$	$E_1^{N,\Delta t}$	2.8318e-01	1.6957e-01	7.6240e-02	2.5064e-02	6.3611e-03
	$R_1^{N,\Delta t}$	0.739	1.153	1.604	1.978	
	$E_2^{N,\Delta t}$	1.0499e-01	5.5195e-02	2.0617e-02	5.5727e-03	1.3576e-03
	$R_2^{N,\Delta t}$	0.927	1.420	1.887	2.037	

TABLE 2.4: Uniform errors $\mathbf{E}^{N,\Delta t}$ and uniform convergence rates $\mathbf{R}^{N,\Delta t}$ using generalized Shishkin mesh for Example 2.2.

Schemes		$N=32$ $\Delta t=1/4$	$N=64$ $\Delta t=1/4^2$	$N=128$ $\Delta t=1/4^3$	$N=256$ $\Delta t=1/4^4$	$N=512$ $\Delta t=1/4^5$
$\boldsymbol{P}_{i,j}=diag(\boldsymbol{A}_{i,j})$	$E_1^{N,\Delta t}$	2.2795e-01	1.6056e-01	7.4906e-02	2.4873e-02	6.3341e-03
	$R_1^{N,\Delta t}$	0.505	1.100	1.590	1.973	
	$E_2^{N,\Delta t}$	2.9137e-01	7.3853e-02	2.0584e-02	5.6177e-03	1.2545e-03
	$R_2^{N,\Delta t}$	1.980	1.843	1.873	2.162	
$\boldsymbol{P}_{i,j}=ltr(\boldsymbol{A}_{i,j})$	$E_1^{N,\Delta t}$	2.2780e-01	1.6049e-01	7.4881e-02	2.4866e-02	6.3324e-03
	$R_1^{N,\Delta t}$	0.505	1.099	1.590	1.973	
	$E_2^{N,\Delta t}$	2.9124e-01	7.3825e-02	2.0584e-02	5.6175e-03	1.2545e-03
	$R_2^{N,\Delta t}$	1.980	1.842	1.873	2.162	
$\boldsymbol{P}_{i,j}=\boldsymbol{A}_{i,j}$	$E_1^{N,\Delta t}$	2.8314e-01	1.6957e-01	7.6240e-02	2.5064e-02	6.3611e-03
	$R_1^{N,\Delta t}$	0.739	1.153	1.604	1.978	
	$E_2^{N,\Delta t}$	1.0471e-01	5.5195e-02	2.0617e-02	5.5727e-03	1.2445e-03
	$R_2^{N,\Delta t}$	0.923	1.420	1.887	2.162	

TABLE 2.5: Uniform errors $\mathbf{E}^{N,\Delta t}$ and uniform convergence rates $\mathbf{R}_{\star}^{N,\Delta t}$ using Shishkin mesh with $N=512$ for Example 2.2.

Schemes		$M=8$	$M=16$	$M=32$	$M=64$	$M=128$
$\boldsymbol{P}_{i,j}=diag(\boldsymbol{A}_{i,j})$	$E_1^{N,\Delta t}$	6.0429e-02	3.0507e-02	1.5333e-02	7.6843e-03	3.8438e-03
	$R_{1,\star}^{N,\Delta t}$	0.986	0.992	0.996	0.999	
	$E_2^{N,\Delta t}$	1.4709e-01	7.3855e-02	3.7000e-02	1.8518e-02	9.2632e-03
	$R_{2,\star}^{N,\Delta t}$	0.993	0.997	0.998	0.999	
$\boldsymbol{P}_{i,j}=ltr(\boldsymbol{A}_{i,j})$	$E_1^{N,\Delta t}$	6.0431e-02	3.0509e-02	1.5335e-02	7.6866e-03	3.8458e-03
	$R_{1,\star}^{N,\Delta t}$	0.986	0.992	0.996	0.999	
	$E_2^{N,\Delta t}$	1.4690e-01	7.3761e-02	3.6953e-02	1.8494e-02	9.2512e-03
	$R_{2,\star}^{N,\Delta t}$	0.993	0.997	0.998	0.999	
$\boldsymbol{P}_{i,j}=(\boldsymbol{A}_{i,j})$	$E_1^{N,\Delta t}$	3.5653e-02	1.8661e-02	9.5779e-03	4.8533e-03	2.4421e-03
	$R_{1,\star}^{N,\Delta t}$	0.933	0.962	0.980	0.990	
	$E_2^{N,\Delta t}$	5.2871e-02	2.6603e-02	1.3343e-02	6.6822e-03	3.3437e-03
	$R_{2,\star}^{N,\Delta t}$	0.990	0.995	0.997	0.998	

TABLE 2.6: Uniform errors $\mathbf{E}^{N,\Delta t}$ and uniform convergence rates $\mathbf{R}_{\star}^{N,\Delta t}$ using generalized Shishkin mesh with $N = 512$ for Example 2.2.

Schemes		$M = 8$	$M = 16$	$M = 32$	$M = 64$	$M = 128$
$\boldsymbol{P}_{i,j} = diag(\boldsymbol{A}_{i,j})$	$E_1^{N,\Delta t}$	5.7355e-02	2.8979e-02	1.4574e-02	7.3083e-03	3.6589e-03
	$R_{1,\star}^{N,\Delta t}$	0.984	0.991	0.995	0.998	
	$E_2^{N,\Delta t}$	1.4690e-01	7.3761e-02	3.6953e-02	1.8494e-02	9.2512e-03
	$R_{2,\star}^{N,\Delta t}$	0.993	0.971	0.998	0.999	
$\boldsymbol{P}_{i,j} = ltr(\boldsymbol{A}_{i,j})$	$E_1^{N,\Delta t}$	6.1556e-02	3.1064e-02	1.5610e-02	7.8230e-03	3.6589e-03
	$R_{1,\star}^{N,\Delta t}$	0.986	0.992	0.996	0.999	
	$E_2^{N,\Delta t}$	1.4560e-01	7.3105e-02	3.6624e-02	1.8329e-02	9.1687e-03
	$R_{2,\star}^{N,\Delta t}$	0.993	0.997	0.998	0.999	
$\boldsymbol{P}_{i,j} = (\boldsymbol{A}_{i,j})$	$E_1^{N,\Delta t}$	3.2559e-02	1.7139e-02	8.7984e-03	4.4608e-03	2.2463e-03
	$R_{1,\star}^{N,\Delta t}$	0.925	0.961	0.979	0.989	
	$E_2^{N,\Delta t}$	5.2593e-02	2.6460e-02	1.3271e-02	6.6458e-03	3.3255e-03
	$R_{2,\star}^{N,\Delta t}$	0.991	0.995	0.997	0.998	

TABLE 2.7: Maximum errors using scheme (2.16)-(2.17) with $\boldsymbol{P}_{i,j} = diag(\boldsymbol{A}_{i,j})$ on Shishkin mesh taking $N = 128$ and $M = 64$ for Example 2.2.

		$\varepsilon_1 = 10^{-1}$	$\varepsilon_1 = 10^{-2}$	$\varepsilon_1 = 10^{-3}$	$\varepsilon_1 = 10^{-4}$	$\varepsilon_1 = 10^{-5}$
$\varepsilon_2 = 10^{-1}$	$E_1^{N,\Delta t}$	4.8356e-03	5.0967e-03	9.0856e-03	5.7620e-02	5.6544e-02
	$E_2^{N,\Delta t}$	8.2690e-03	1.0405e-02	1.0720e-02	1.0744e-02	1.0734e-02
$\varepsilon_2 = 10^{-2}$	$E_1^{N,\Delta t}$	*	7.2798e-02	7.0729e-02	6.2050e-02	5.7983e-02
	$E_2^{N,\Delta t}$	*	1.7957e-02	1.7896e-02	1.7895e-02	1.7895e-02
$\varepsilon_2 = 10^{-3}$	$E_1^{N,\Delta t}$	*	*	7.5923e-02	7.4630e-02	6.2262e-02
	$E_2^{N,\Delta t}$	*	*	1.8339e-02	1.8334e-02	1.8330e-02
$\varepsilon_2 = 10^{-4}$	$E_1^{N,\Delta t}$	*	*	*	2.6420e-02	2.4821e-02
	$E_2^{N,\Delta t}$	*	*	*	2.0578e-02	1.8451e-02
$\varepsilon_2 = 10^{-5}$	$E_1^{N,\Delta t}$	*	*	*	*	2.6461e-02
	$E_2^{N,\Delta t}$	*	*	*	*	2.0582e-02

TABLE 2.8: Maximum errors using scheme (2.16)-(2.17) with $\boldsymbol{P}_{i,j} = ltr(\boldsymbol{A}_{i,j})$ on Shishkin mesh taking $N = 128$ and $M = 64$ for Example 2.2.

		$\varepsilon_1 = 10^{-1}$	$\varepsilon_1 = 10^{-2}$	$\varepsilon_1 = 10^{-3}$	$\varepsilon_1 = 10^{-4}$	$\varepsilon_1 = 10^{-5}$
$\varepsilon_2 = 10^{-1}$	$E_1^{N,\Delta t}$	4.8582e-03	5.1152e-03	9.0916e-03	5.7654e-02	5.6548e-02
	$E_2^{N,\Delta t}$	8.2178e-03	1.0361e-02	1.0698e-02	1.0751e-02	1.0735e-02
$\varepsilon_2 = 10^{-2}$	$E_1^{N,\Delta t}$	*	7.2915e-03	7.0822e-02	6.2404e-02	5.8018e-02
	$E_2^{N,\Delta t}$	*	1.8756e-02	1.7895e-02	1.7895e-02	1.7895e-02
$\varepsilon_2 = 10^{-3}$	$E_1^{N,\Delta t}$	*	*	7.9933e-02	7.8073e-02	6.2617e-02
	$E_2^{N,\Delta t}$	*	*	2.8112e-02	2.7869e-02	1.8330e-02
$\varepsilon_2 = 10^{-4}$	$E_1^{N,\Delta t}$	*	*	*	2.9074e-02	2.8270e-02
	$E_2^{N,\Delta t}$	*	*	*	4.2641e-02	2.7902e-02
$\varepsilon_2 = 10^{-5}$	$E_1^{N,\Delta t}$	*	*	*	*	2.9118e-02
	$E_2^{N,\Delta t}$	*	*	*	*	2.4004e-02

TABLE 2.9: The CPU time (in seconds) using Shishkin mesh for Example 2.1 with $\varepsilon_1 = 10^{-8}$, $\varepsilon_2 = 10^{-7}$.

Schemes	$N = 32$ $\Delta t = 1/4^1$	$N = 64$ $\Delta t = 1/4^2$	$N = 128$ $\Delta t = 1/4^3$	$N = 256$ $\Delta t = 1/4^4$	$N = 512$ $\Delta t = 1/4^5$
$\boldsymbol{P}_{i,j} = diag(\boldsymbol{A}_{i,j})$	0.651	3.793	31.856	400.168	6339.446
$\boldsymbol{P}_{i,j} = \boldsymbol{A}_{i,j}$	0.683	4.526	51.817	814.021	12612.586

TABLE 2.10: The CPU time (in seconds) using generalized Shishkin mesh for Example 2.1 with $\varepsilon_1 = 10^{-8}$, $\varepsilon_2 = 10^{-7}$.

Schemes	$N = 32$ $\Delta t = 1/4^1$	$N = 64$ $\Delta t = 1/4^2$	$N = 128$ $\Delta t = 1/4^3$	$N = 256$ $\Delta t = 1/4^4$	$N = 512$ $\Delta t = 1/4^5$
$\boldsymbol{P}_{i,j} = diag(\boldsymbol{A}_{i,j})$	0.569	3.632	31.221	392.012	6287.464
$\boldsymbol{P}_{i,j} = \boldsymbol{A}_{i,j}$	0.771	4.724	47.911	847.955	12560.541

TABLE 2.11: The CPU time (in seconds) using Shishkin mesh for Example 2.2 with $\varepsilon_1 = 10^{-8}$, $\varepsilon_2 = 10^{-7}$

Schemes	$N = 32$ $\Delta t = 1/4^1$	$N = 64$ $\Delta t = 1/4^2$	$N = 128$ $\Delta t = 1/4^3$	$N = 256$ $\Delta t = 1/4^4$	$N = 512$ $\Delta t = 1/4^5$
$\boldsymbol{P}_{i,j} = diag(\boldsymbol{A}_{i,j})$	0.336	1.229	8.229	65.718	676.488
$\boldsymbol{P}_{i,j} = \boldsymbol{A}_{i,j}$	0.351	1.293	8.732	86.521	1071.031

TABLE 2.12: The CPU time (in seconds) using generalized Shishkin mesh for Example 2.2 with $\varepsilon_1 = 10^{-8}$, $\varepsilon_2 = 10^{-7}$.

Schemes	$N = 32$ $\Delta t = 1/4^1$	$N = 64$ $\Delta t = 1/4^2$	$N = 128$ $\Delta t = 1/4^3$	$N = 256$ $\Delta t = 1/4^4$	$N = 512$ $\Delta t = 1/4^5$
$\boldsymbol{P}_{i,j} = diag(\boldsymbol{A}_{i,j})$	0.266	1.206	8.281	64.284	657.262
$\boldsymbol{P}_{i,j} = \boldsymbol{A}_{i,j}$	0.281	1.288	8.967	84.469	1077.065

and convergence rates taking $N = 512$ for Example 2.2 in Tables 2.5 and 2.6. In these tables the uniform convergence rates are computed as follows

$$\mathbf{R}_{\star}^{N,\Delta t} = \log_2(\mathbf{E}^{N,\Delta t}/\mathbf{E}^{N,\Delta t/2}).$$

One can observe that these numerical results are in line with the theory. Further, Tables 2.7 and 2.8 display the maximum errors fixing $N = 128$ and $M = 64$ and using different values of ε_1 and ε_2 for Example 2.2. Here, $\star$ is used to denote that the condition $0 < \varepsilon_1 \leq \varepsilon_2 \leq 1$ is not satisfied. In Tables 2.9 and 2.10 we give the CPU time (in seconds) to compare the computational cost taking $\varepsilon_1 = 10^{-8}$, $\varepsilon_2 = 10^{-7}$ for Example 2.1. The results show that the choice $\boldsymbol{P}_{i,j} = diag(\boldsymbol{A}_{i,j})$ requires less time in comparison to the choice $\boldsymbol{P}_{i,j} = \boldsymbol{A}_{i,j}$. Further, we observe during the experiments that the CPU time for $\boldsymbol{P}_{i,j} = ltr(\boldsymbol{A}_{i,j})$ and $\boldsymbol{P}_{i,j} = diag(\boldsymbol{A}_{i,j})$ is similar. Similar results for Example 2.2 are given in Tables 2.11 and 2.12.

In summary although all the choices have similar uniform errors and the uniform

convergence rates, the splitting schemes $\boldsymbol{P}_{i,j} = diag(\boldsymbol{A}_{i,j})$ and $\boldsymbol{P}_{i,j} = ltr(\boldsymbol{A}_{i,j})$ are computationally more efficient than the classical implicit Euler scheme $\boldsymbol{P}_{i,j} = \boldsymbol{A}_{i,j}$ [52].

2.5 Conclusions

In this work, we have developed a computationally efficient numerical method for solving the coupled system of singularly perturbed delay parabolic problems (2.1). The numerical method constitutes two splitting schemes on uniform meshes for time discretization and the central difference scheme on Shishkin and generalised Shishkin meshes for space discretization. The proposed numerical method is shown to be uniformly convergent of order one in time and almost two in space. Further, it is computationally more efficient than the standard numerical method. Numerical results are given to illustrate the efficiency of the splitting schemes.

****